Materials Transactions, Vol. 44, No. 2 (2003) pp. 259 to 267

Electro-Deposition of Tantalum on Tungsten and Nickel in LiF–NaF–CaF_2 Melt Containing K_2TaF_7—Electrochemical Study

Mazhar Mehmood[1,2], Nobuaki Kawaguchi[1], Hideki Maekawa[1], Yuzuru Sato[1], Tsutomu Yamamura[1], Masayoshi Kawai[3] and Kenji Kikuchi[4]

[1]*Department of Metallurgy, Graduate School of Engineering, Tohoku University, Sendai 980-8579, Japan*
[2]*Permanent: Pakistan Institute of Engineering and Applied Sciences, Islamabad, Pakistan*
[3]*High Energy Accelerator Research Organization, Tsukuba 305-0801, Japan*
[4]*Japan Atomic Energy Research Institute, Tokai, Ibaraki 319-1195, Japan*

Electrochemical study has been carried out on the electro-deposition of tantalum in 55 mol%LiF–35 mol%NaF–10 mol%CaF_2 melt containing 1–2 mol%K_2TaF_7 at 700°C. This has been done for determining the mechanistic features for preparing electrolytic coating of tantalum on nickel and tungsten substrates. Electro-deposition of metallic tantalum occurs primarily by electro-reduction of Ta(V), *i.e.*, TaF_7^{2-} at a potential of < -0.5 V (vs. nickel used as a quasi reference electrode). At potentials < -0.55 V, $TaOF_5^{2-}$ also undergoes reduction to form metallic tantalum. The oxide ions generated by reduction of $TaOF_5^{2-}$ are removed from the surface by an oxide ion getter in the LiF–NaF–CaF_2 melt. Pure metallic tantalum without any entrapped salt is successfully deposited on tungsten by galvanostatic polarization at reasonably low current densities. An additional feature on nickel is the formation of an intermetallic compound at potential ~0.25 V nobler than that of pure tantalum as a result of underpotential deposition of tantalum. This intermetallic compound covers the surface within a short time followed by deposition of pure tantalum, although intermetallic compound keeps growing at the interface of pure tantalum deposit and the substrate as a result of diffusion. Other secondary reactions are (i) a low activity reduction of Ta(V) to Ta(II) at −0.25 V, (ii) a conproportionation reaction at the surface of electrode leading to partial dissolution of tantalum and, (iii) a corresponding disproportionation reaction that forms powdery metallic tantalum at the salt surface.

(Received October 3, 2002; Accepted December 16, 2002)

Keywords: *tantalum, coating, electro-deposition, molten salt, intermetallic compound, nickel, tungsten*

1. Introduction

Tantalum exhibits high corrosion resistance in a wide range of aggressive media. It has high thermal & electric conductivity and excellent fabricability among valve metals.[1)] However, its use as a structural material is difficult due to high density and cost.

The most interesting characteristics of tantalum are the surface properties. These can be benefited by employing tantalum coating on a base metal or alloy that best fits with the engineering requirements in a cost-effective manner. For instance, the amorphous and nanocrystalline valve-metal alloy coatings exhibit extremely high corrosion resistance in concentrated HCl.[2–5)] Among these, the highest corrosion resistance is observed for tantalum-based alloys.[2)] Similarly, tantalum coatings have been effective in protection of steel against high temperature wear and erosion.[6,7)] The tantalum coatings have also proved suitable as substrate in dimensionally stable anodes for oxygen evolution.[8)]

Among various techniques used for preparing coatings, electro-deposition is extremely useful due to low cost and high flexibility for big size and complicated shape of the objects to be coated.

Molten salt electrolysis has been successfully applied for deposition of valve metals[9)] and their alloys.[10,11)] Nevertheless, a compact coating is usually difficult and requires strict control on quality of the salt and environment of the reaction chamber primarily due to oxide-ion effect, disproportionation reactions, etc.[9,12–15)]

The presence of oxide ions in LiF–NaF or LiF–NaF–KF melts is known for deteriorating the quality of coating due to formation of oxyfluorotantalates.[14,15)] The electro-reduction of oxyfluorotantalate leads to the formation of oxides of tantalum instead of metallic tantalum as observed by Chamelot *et al.*[15)] Recently, Kawaguchi *et al.*[16,17)] have found similar results when deposition was tried at a potential sufficiently negative to reduce the oxyfluorotantalates present in the LiF–NaF melt. They found tantalum containing oxides in the electrodeposits. By contrast, the deposition under similar conditions in LiF–NaF melt containing 10%CaF_2 resulted in formation of metallic tantalum instead of tantalum oxides. Although the deposit contained entrapped salt due to dendritic growth at active potentials and high current density, the beneficial role of CaF_2 was well established.

Hence, attempt to prepare compact and coherent tantalum coatings in this melt may be interesting. This should provide more flexibility on the control of salt quality and environment of the reaction chamber as a result of more tolerance against oxyfluorotantalate ions. Presently we are working for exploring the possibility of coherent and compact coating of tantalum on tungsten and nickel substrates in the melt containing CaF_2.

Our interest in coating on tungsten is partly based on its selection as a proposed solid target for high-energy neutron generation.[18)] The tungsten target has to be coated by tantalum in order to provide protection against wear and corrosion caused by cooling water with high flow rate at high temperatures.[18,19)]

On the other hand, nickel is an interesting engineering material for its high temperature structural applications. Its use as an intermediate coating for 'difficult to coat' substrates is also quite popular. Taxil *et al.* have presented results on tantalum coating on nickel in LiF–NaF melt. However, the quality of coating at the interface was not good due to which

Taxil *et al.* encountered flaking during electro-deposition.[20] A good coating of pure tantalum may enhance its applications in severe corrosive environments or where slight corrosion is not tolerable, in addition to facilitating tantalum coating on 'difficult to coat' substrates as an undercoat.

The present paper is meant for reporting the electrochemical study that has been conducted in order to understand the mechanistic aspects of electro-deposition on tungsten and nickel substrates in LiF–NaF–CaF_2 melt.

2. Experimental Procedures

Analytical grade LiF and CaF_2 were purchased from Kanto Chemical and analytical grade NaF from Wako Pure Chemicals. K_2TaF_7 was provided by Showa Cabot Supermetals Co. The chemicals were used without any further processing.

The cell consisted of a graphite or nickel crucible, a graphite rod as counter electrode, a nickel rod as reference electrode, and a tungsten or nickel wire as working electrode.

A vertical stainless steel tube lined with Mullite tube was used as reaction chamber. The upper part was cooled with water. The crucible was placed in the reaction tube, while the electrodes extended to outside the reaction tube through holes in the lid. All the openings were provided with seats for silicone rubber to isolate the chamber to make it leak proof. The temperature of the chamber was measured at a few centimetres above the salt with the help of an R-type thermocouple. The temperature was controlled within 0.5 K by a thermostat (Chino, Model DB).

The preparation for the experiments was performed as follows. The salts were mixed in the required ratio. After placing the crucible along with the salt mixture and adjusting the electrodes in the chamber, the chamber was evacuated and the temperature was raised to 200°C. At this temperature a vacuum drying was carried out for a period of about 24 h. After that the chamber was filled with dry argon and temperature was raised very slowly to 450°C at which overnight drying was carried out under argon flow. The temperature was then slowly raised to the working temperature.

The experiments were performed at 700°C under argon flow. The electrochemical measurements were performed with the help of a function generator (Hokuto HB-104), a galvanostat / potentiostat (Hokuto HA-305) and a recorder (Rikadai IL-025). For the characterization of electro-deposits, scanning electron microanalyzer (Hitachi, Model X-650) was used.

3. Results

Figure 1(a) shows a typical cyclic voltammogram obtained on the nickel electrode in the 55LiF–35NaF–10CaF_2 melt containing 1%K_2TaF_7 at a sweep rate of 0.1 $V \cdot s^{-1}$. (The electrolyte composition is given in mole percent. If not mentioned otherwise, the same composition is used throughout the experiments.) Four cathodic waves are detected on these voltammograms, *i.e.*, marked as R_1, R_2, R_3 and R_4. The peak potentials are approximately −0.26 V and −0.28 V for the first two waves. The peak potential for wave R_3 is not very clear. However, it is close to −0.54 V. The peak potential for the wave R_4 is below −0.6 V. As shown in Fig. 1(b), the shapes and the current densities of the waves R_3 and R_4 obtained on tungsten are similar to those obtained on nickel. Hence, there is no difference of cathodic processes taking place on nickel and tungsten electrodes at potential below −0.5 V.

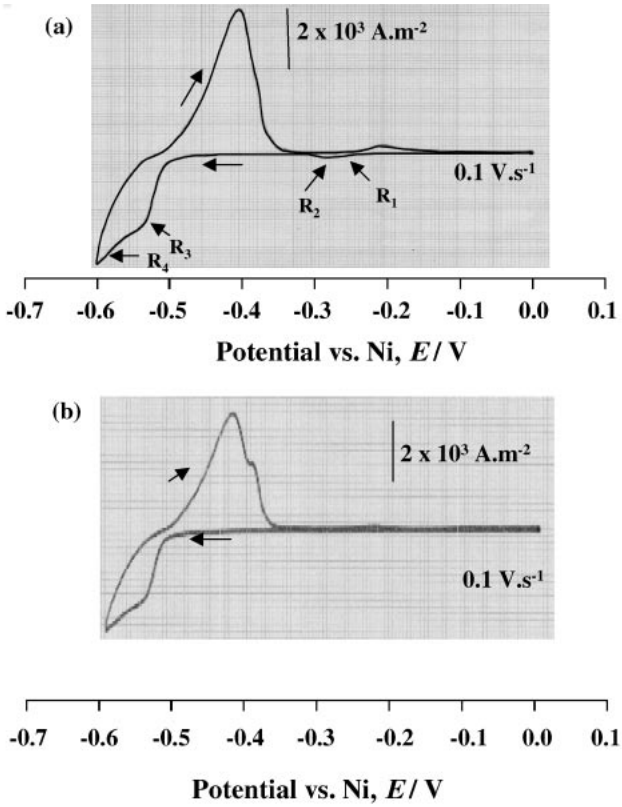

Fig. 1 Typical voltammograms obtained on nickel (a) and tungsten (b) electrodes in 55LiF–35NaF–10CaF_2 melt containing 1%K_2TaF_7 at 700°C. The sweep rate was 0.1 $V \cdot s^{-1}$. The voltammograms were obtained by cathodic polarization from open circuit potential, followed by anodic polarization to the same potential.

At higher resolution of current, the voltammograms obtained on tungsten show a wave at ~ -0.26 V similar to R_1 observed on nickel, as shown in Fig. 2. On the other hand, the wave R_2 does not appear on tungsten.

In order to clarify the nature of reaction taking place at R_1 and R_2, voltammograms were obtained on nickel at a narrow range of potential, as shown in Fig. 3. Two separate cathodic waves *i.e.*, R_1 and R_2, (and corresponding anodic waves, O_1 and O_2) are clearly identified particularly at low polarization rates. The current density is higher in case of the electrolyte containing 2%K_2TaF_7 in comparison with that containing 1%K_2TaF_7. Hence, the waves are related with redox processes of tantalum. The peak position changes with polarization rate with an accompanied overlap. The peak position of O_1 wave does not change with polarization rate. On the other hand, a negative shift in the peak position takes place for R_1 wave. This shift is primarily due to changes in background current of the wave R_2. Even in this case, peak position of R_1 wave does not change significantly at polarization rates less than 0.2 $V \cdot s^{-1}$. Accordingly, the reaction that takes place at R_1 and O_1 is reversible at low

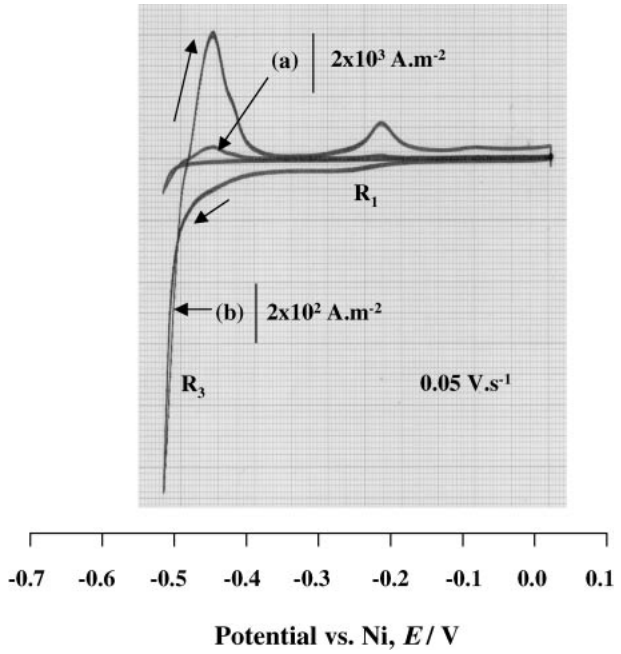

Fig. 2 A voltammogram obtained on tungsten electrode in 55LiF–35NaF–10CaF_2 melt containing 1%K_2TaF_7 at 700°C. The sweep rate was 0.05 V·s^{-1}. The (a) and (b) were obtained under similar conditions, except that the current was measured at a higher resolution in case of (a).

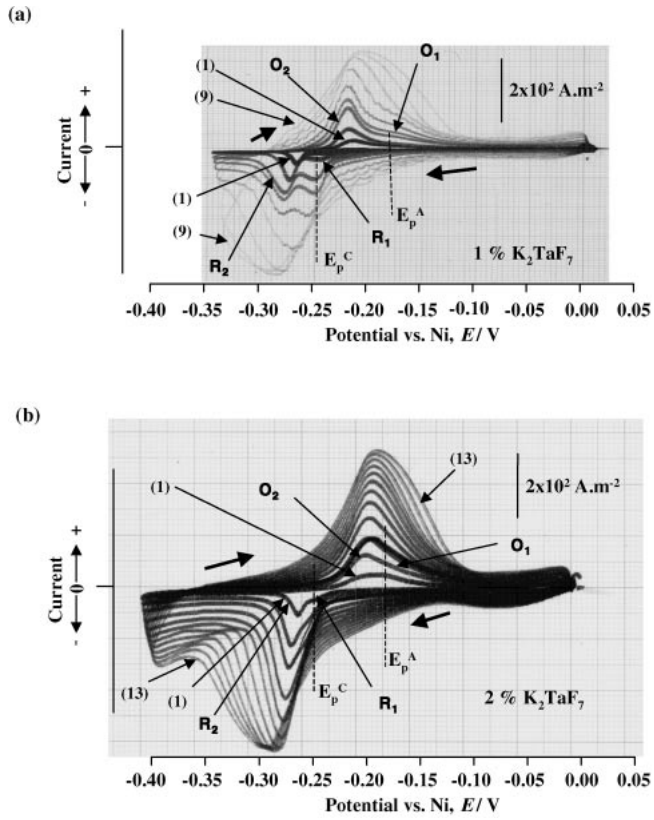

Fig. 3 Voltammograms obtained on nickel in 55LiF–35NaF–10CaF_2 melt at 700°C. (a): The melt contained 1%K_2TaF_7; The voltammograms from (1) to (9) were obtained at sweep rates of 0.002, 0.01, 0.05, 0.1, 0.2, 0.4, 0.6, 0.8, 1.0 V·s^{-1}. (b): The melt contained 2%K_2TaF_7; The voltammograms from (1) to (13) were obtained at sweep rates of 0.005, 0.01, 0.05, 0.1, 0.2, 0.3, 0.4, 0.5, 0.6, 0.7, 0.8, 0.9, 1.0 V·s^{-1}.

polarization rates.

The charge transfer number (n) for a reversible redox process can be calculated by using eq. (1):[22]

$$E_p^A - E_p^C = 2.3RT/nF \quad (1)$$

where $E_p^A - E_p^C$ is the difference between peak potentials of anodic and cathodic waves; R, T and F are gas constant, temperature and Faraday's constant, respectively. The difference in peak positions ($E_p^A - E_p^C$) between R_1 and O_1 waves at low sweep rates is 0.065 to 0.070 V. This difference is similar when voltammograms are obtained on tungsten at low polarization rate. The charge transfer number (n) of the reaction taking place at R_1 is 2.97 if calculated by taking the value of $E_p^A - E_p^C$ equal to 0.065 V. Hence, the charge transfer number appears to be 3. This is in agreement with that observed by Senderoff *et al.* for the first step of Ta(V) reduction in eutectic LiF–NaF–KF melt.[21] Accordingly, the reaction at R_1 can be described by eq. (2).

$$Ta(V) + 3e^- = Ta(II) \quad (2)$$

An interesting feature of Fig. 3 is the very narrow widths of R_2 and O_2 peaks at low polarization rates. For instance, width of the peak at half of its maximum value (FWHM) for the R_2 wave in Fig. 3(a) at a polarization rate of 0.002 V·s^{-1} is only ~0.015 V. The very small width is typical for redox waves involving an adsorbed oxidant or product,[22] the typical shape being associated with the formation of barrier between reductant and substrate surface that stops or slows down further reaction. The situation should be similar if a thin layer of intermetallic compound is formed. These considerations, in addition to the fact that R_2 wave is observed only on nickel, clearly suggest that it is related with the formation of an intermetallic compound between nickel and tantalum as a result of underpotential deposition of tantalum.

No other wave on nickel can be related with formation of an intermetallic compound since they are also observed on tungsten. Hence, only one intermetallic compound is formed by underpotential deposition of tantalum.

In order to understand the nature of wave R_3, reverse chronopotentiometry was carried out. Figure 4 shows cyclic chronopotentiograms obtained on tungsten as a function of current density. At a current density of about 2.3×10^2 A·m^{-2}, the electrode potential comes to the region of R_3 shortly after the cathodic current is applied. It can be noted in Fig. 4(a) that reduction process continues for about 5.7 s at a cathodic current of 2.3×10^2 A·m^{-2}. When the direction of the current is reversed, the time required for re-oxidizing the reductant is about 4 s. Hence, the ratio of the time required for re-oxidizing to the time spent for making the reductant (T_{ox}/T_{red}) is approximately 70%. A decrease in T_{ox}/T_{red} occurs with lowering the applied current density. As shown in Fig. 4(c), T_{ox}/T_{red} is approximately 40% for a current density of 50 A·m^{-2}. It is known that the T_{ox}/T_{red} should be close to 33% if the direction of the current is reversed after forming a soluble reductant since most of the reductant diffuses away from the electrode and cannot return to the electrode to re-oxidize.[22] Hence, the reductant formed prior to wave R_3 is almost soluble as the time required for its oxidation is much less than the time for charging. As the

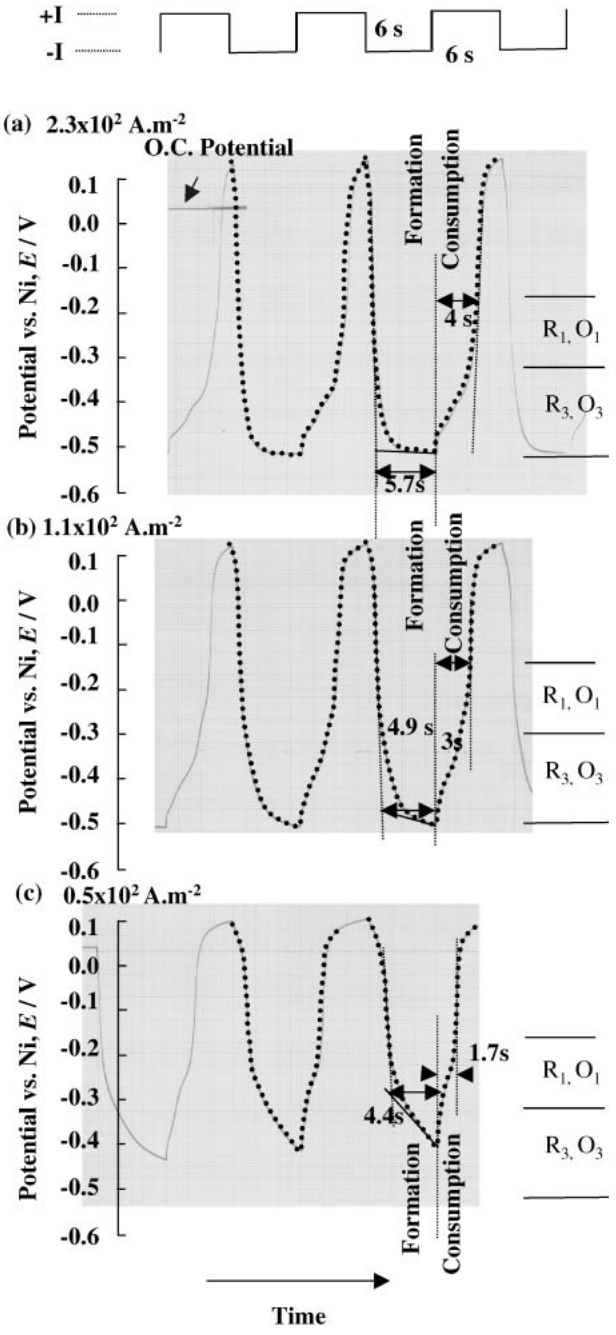

Fig. 4 Cyclic chronopotentiograms obtained on tungsten in LiF–NaF–CaF_2 containing 1%K_2TaF_7 at 700°C. The approximate positions of waves in the voltammograms have been indicated along with the chronopotentiograms.

current density is increased, the electrode potential stays below −0.5 V in the region of R_3 for a reasonable length of time. This results in an increase in the T_{ox}/T_{red}. This reveals that the reductant formed at wave R_3 (Fig. 1) is insoluble, although completely insoluble nature is not confirmed by this method. It can be noticed from the chronopotentiograms that two anodic plateaus are observed in the region of R_3 and O_3, although only one cathodic plateau is seen. This aspect will be emphasized later.

In order to determine the nature of the product formed at R_3, galvanostatic polarization was carried out on tungsten at a current density of -2×10^2 A·m^{-2}. The potential remained in the region of wave R_3 during electro-deposition. Figure 5

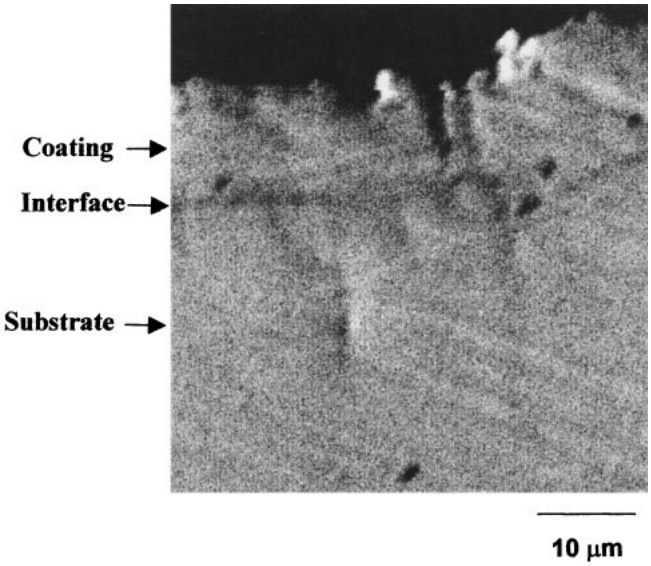

Fig. 5 Cross-sectional view of tungsten electrode after electro-deposition at −20 mA·cm^{-2}.

shows the cross-section of the electrode. A solid is retained on the electrode. The characteristic X-ray spectra obtained from the substrate and the deposit are shown in Figs. 6(a) and (b), respectively. All the peaks observed from the deposit belong to tantalum. Hence, the deposition of metallic tantalum takes place at wave R_3, although the interface of the deposit and the substrate is not satisfactory. No diffusion of tantalum into substrate is observed, as characteristic X-rays are totally absent in the X-ray spectrum obtained from the substrate.

Although Ta(II) is formed prior to R_3, its concentration should be very low as indicated by the low height of the wave R_1. Accordingly, the wave R_3 corresponds to the reduction of Ta(V) to Ta(0) as shown in eq. (3).

$$TaF_7^{2-} + 5e^- = Ta + 7F^- \quad (3)$$

In order to understand the nature of wave R_4, cyclic voltammograms were obtained in electrolyte containing 2% K_2TaF_7. The current densities of both R_3 and R_4 are higher than those obtained in the electrolyte containing 1%K_2TaF_7 (Fig. 1). Hence, both the waves are related with redox processes of tantalum. The waves R_3 and R_4 cannot be assumed as sequential steps for reducing Ta(V) to Ta(0) since metallic tantalum is deposited on R_3. This suggests that R_4 should correspond to another parallel process for reducing tantalum.

As shown in Fig. 7, a new anodic wave does not appear at more noble potential when the cathodic sweep extends significantly into the region of wave R_4 from the region of wave R_3. This indicates that the nature of the anodic reaction for the product formed at R_4 is similar to that formed at R_3. Accordingly, the product formed under wave R_4 and retained at the electrode may be the same as the one formed under R_3, *i.e.*, metallic tantalum.

Polyakova *et al.*[14] studied the effect of oxide ions on redox processes of tantalum in LiF–NaF–KF melt and established that reduction of $TaOF_7^{2-}$ occurs at slightly more active potentials than that of TaF_7^{2-} by reaction (4).

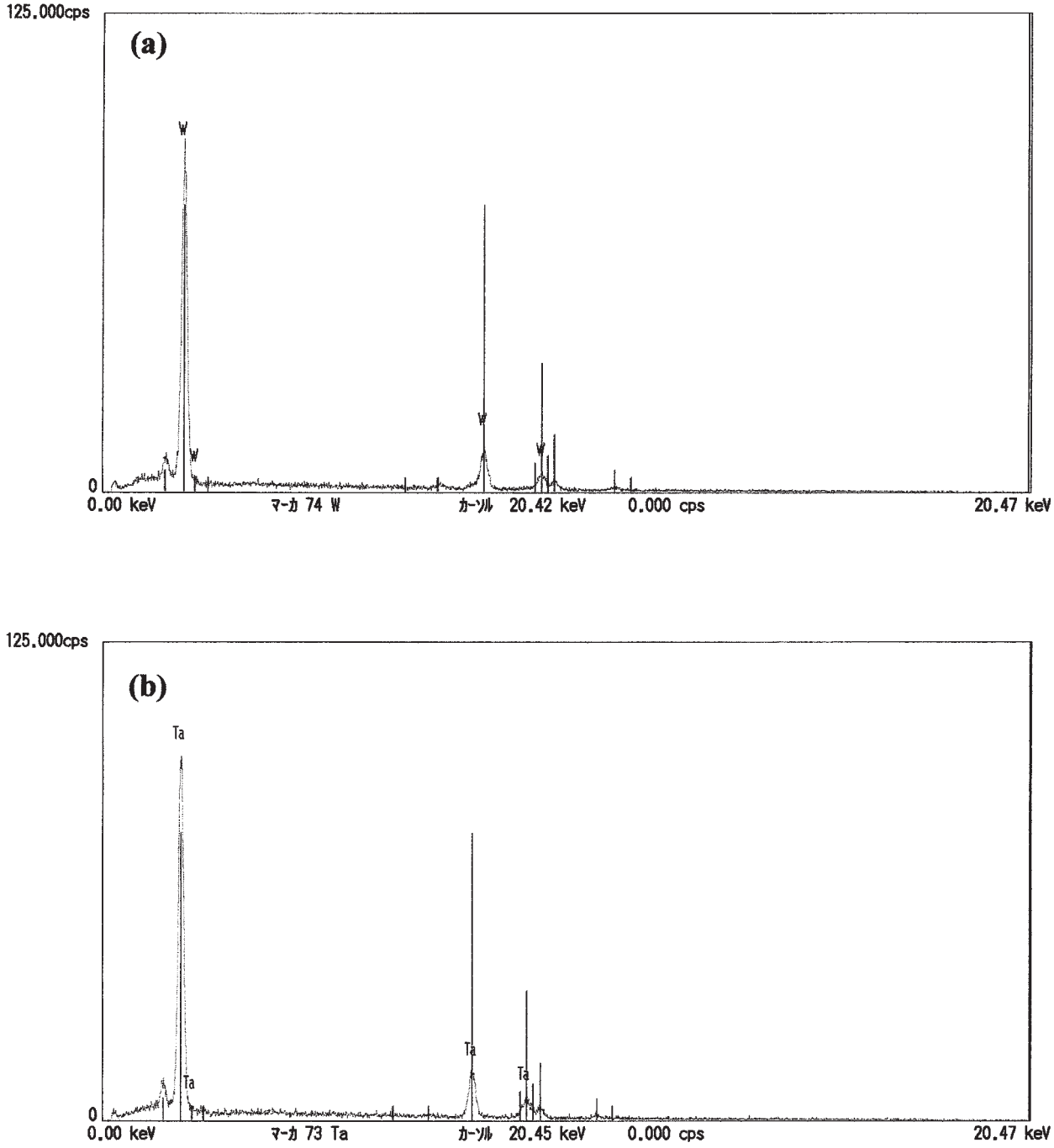

Fig. 6 X-ray spectra obtained from a section of tungsten electrode after electro-deposition at $-20\,mA{\cdot}cm^{-2}$ (a) substrate (b) coating. The positions of characteristic X-rays of tungsten and tantalum are also shown in the form of vertical lines on (a) and (b), respectively. Although the spectra of tungsten and tantalum are close to each other, all the peaks are identified as those of tantalum in the coating and no peak of tantalum is observed in the substrate. The figure indicates the formation of pure tantalum without any alloyed tungsten, in addition to absence of diffusion between coating and substrate.

$$TaOF_5^{2-} + 5e^- = Ta + O^{2-} + 5F^- \quad (4)$$

Hence, wave R_4 corresponds to reduction of oxyfluorotantalate to metallic tantalum by reaction (4).

In contrast to the results of Polyakova *et al.* who found a pair of additional anodic and cathodic waves related with reaction (4) in LiF–NaF–KF melt,[14] we have not observed an anodic wave of the reaction (4) in LiF–NaF–CaF_2 melt. This suggests that metallic tantalum is oxidised by reaction (3) instead of reaction (4) during anodic scan due to unavailability of O^{2-} to form $TaOF_5^{2-}$. It seems to have reacted with an oxygen getter as shown in (5) and (6).

$$O^{2-} + TaF_7^{2-} = TaOF_5^{2-} \quad (5)$$

or

$$Ca^{2+} + O^{2-}(+xF^-) = CaO(F_x^{x-}) \quad (6)$$

Considering very low concentration of TaF_7^{2-} in the vicinity of electrode, the reaction (6) seems to be more probable. The positive role of Ca^{2+} in the molten salt baths due to its high affinity for oxide ion has been clearly

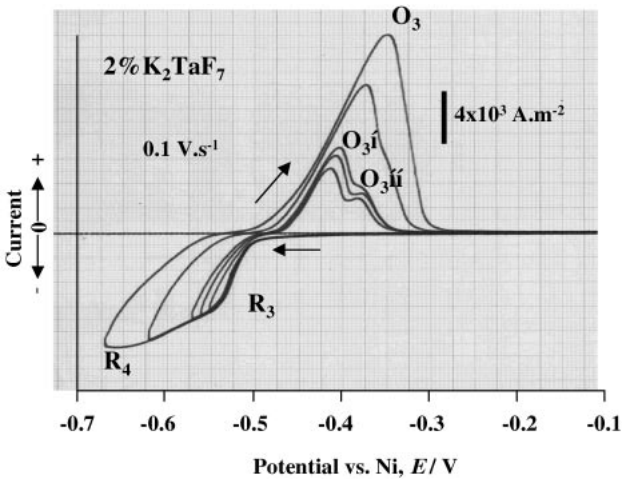

Fig. 7 Cyclic voltammograms obtained on tungsten at a sweep rate of $0.1\,V{\cdot}s^{-1}$. The electrolyte was LiF–NaF–CaF_2 melt containing 2% K_2TaF_7.

demonstrated by Chen *et al.*[23)]

Figure 7 has revealed another interesting fact. It can be noted that the wave O_3 splits into two, *i.e.*, O_3' and O_3'' when the sweep direction is reversed at an early stage under wave R_3. This phenomenon is also found in voltammograms obtained by Taxil *et al.*[20)] who observed two overlapped anodic waves after polarizing through a single cathodic wave; the working electrode was molybdenum and the electrolyte was NaF–LiF melt containing K_2TaF_7. Extra anodic peaks have also been reported in chloride melts.[24)]

These results are in agreement with the reverse chronopotentiometry (Fig. 4) that reveals existence of two anodic plateaus corresponding to a single cathodic plateau due to the formation of metallic tantalum from TaF_7^{2-}. (These two anodic plateaus are always observed independent of the substrate, although their relative width varies with current density). This reveals that another intermediate oxidation state also exists and the dissolution of tantalum proceeds partly through this intermediate specie. A separate cathodic wave is not observed for its formation. Hence, it is probably formed by conproportionation reaction between Ta(0) and Ta(V) during electro-deposition of tantalum.

If electrolysis is carried out for a long duration, thin powdery sludge covers the surface that contains metallic tantalum as revealed by X-ray analysis and conductivity measurements. It appears that the product of conproportionation reaction formed at the electrode surface of electrodeposited tantalum diffuses away, and being unstable in the bulk electrolyte, undergoes disproportionation reaction to form powdery tantalum and Ta(V).

The deposition mechanism on nickel surface is different from that on the tungsten surface due to the formation of an intermetallic compound. Therefore, reverse chronopotentiometry was also carried out on nickel surface as shown in Fig. 8. Two plateaus are observed at $-0.3\,V$ and below $-0.5\,V$ at a current density of $2 \times 10^2\,A{\cdot}m^{-2}$. The former being associated primarily with the underpotential deposition of tantalum in the form of intermetallic compound and the latter for deposition of pure tantalum. As observed in Fig. 8(a), the time for anodic dissolution of intermetallic compound is almost equal to that for its formation when the direction of current is reversed after one second. On the other hand, the time for its dissolution is much longer than that for its formation if the direction of current is reversed to anodic direction after six seconds. This indicates that intermetallic compound is formed not only by underpotential deposition of tantalum at $-0.3\,V$ but it continues to grow by diffusion during deposition of pure tantalum. As shown in Fig. 8(c), three anodic plateaus can be associated with formation of intermetallic compound although only one is

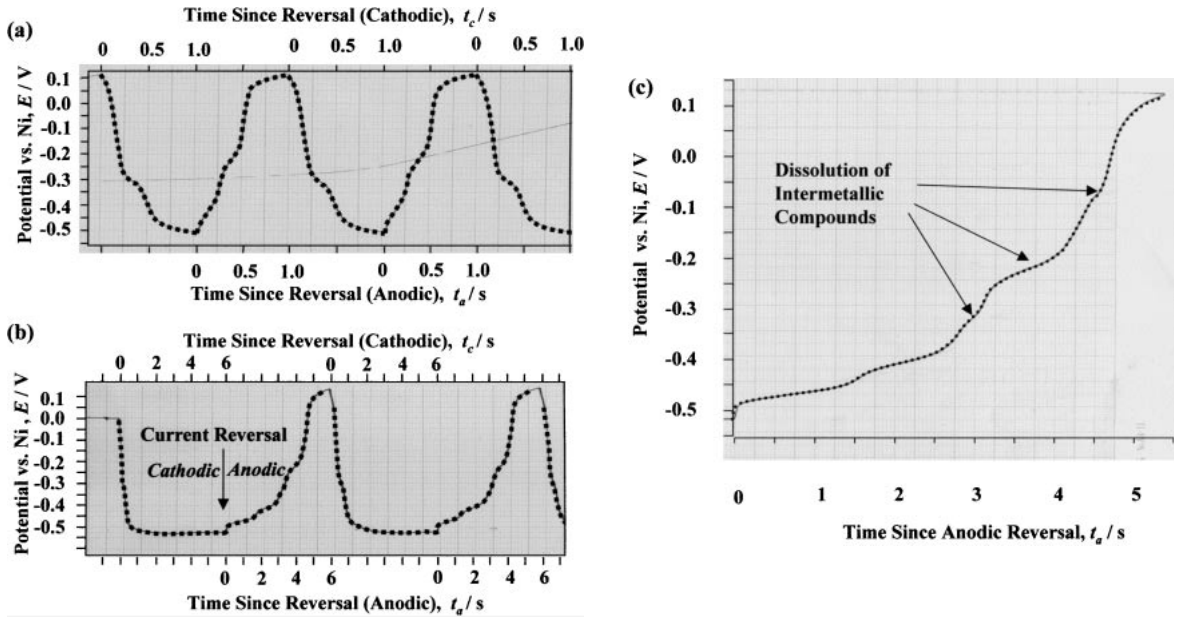

Fig. 8 Chronopotentiograms obtained on nickel in LiF–NaF–CaF_2 melt containing 1%K_2TaF_7 at 700°C (a) Time for dissolution of intermetallic compound is similar to that of formation, (b) the time for dissolution is longer due to growth of intermetallic compound due to diffusion, (c) same as (b) clearly shows the formation a number of intermetallic compound due to diffusion.

formed partly by underpotential deposition of tantalum as detected by cathodic chronopotentiograms and voltammograms. Hence, the remaining two are possibly formed solely by diffusion.

4. Discussion

4.1 Electro-reduction of TaF_7^{2-} (in LiF–NaF–CaF_2 Melt)

Although a reaction with charge transfer number (n) of 3 is observed at potentials nobler than required for deposition of metallic tantalum, its wave exhibits very low current density. Hence, its rate should be extremely small. The major reaction for deposition of metallic tantalum is reduction of TaF_7^{2-} with charge transfer number of 5, as described below

$$TaF_7^{2-}(\text{soln.}) + 5e^- = Ta(\text{coating}) + 7F^-(\text{soln.}) \qquad (A)$$

This reaction takes place at a potential of -0.5 to -0.55 V vs. Ni. This potential is easily achieved and maintained at low current densities.

The mechanism of electro-reduction of Ta(V) has been a matter of considerable debate.[13] In fluoride melts, two step (V to II to 0) and single-step (V to 0) mechanisms have been observed sometimes in the melts apparently having similar composition. However, the presence of oxide may change the nature of tantalum-containing complexes and lead to variation of mechanism from one melt to another. In our melt, both the mechanisms are operative, possibly due to two types of complexes, the one with higher concentration being resistant for two-step reduction.

4.2 Electro-reduction of $TaOF_5^{2-}$

At more negative potentials reduction of $TaOF_5^{2-}$ supplements the reduction of TaF_7^{2-} to form metallic tantalum, as described below,

$$TaOF_5^{2-}(\text{soln.}) + 5e^- = Ta(\text{coating}) + O^{2-}(\text{soln.}) + 7F^-(\text{soln.}) \qquad (B)$$

Polyakova *et al.*[14] have investigated the effect of oxide ion addition on the electro-reduction of Ta(V). They found new pairs of reduction and oxidation waves after the formation of $TaOF_5^{2-}$, and $TaO_2F_3^{2-}$, etc. The presence of anodic wave for each oxyfluoride indicated the anodic reaction of type (B) because of the presence of O^{2-} in the vicinity of the electrode. Chamelot *et al.*[15] have advocated that TaO is formed instead of metallic tantalum as a result of reduction of $TaOF_5^{2-}$. In such a case, a separate anodic wave for oxidation of TaO to $TaOF_5^{2-}$ should appear.

By contrast, we have not observed a separate anodic wave for the reaction (B) or oxidation of TaO to $TaOF_5^{2-}$ indicating that O^{2-} produced by reduction of $TaOF_5^{2-}$ has been combined with an oxide ion getter in the electrolyte in an irreversible manner. The possible candidates for capturing O^{2-} ions are TaF_7^{2-} and Ca^{2+}. Since $TaOF_7^{2-}$ exists in the electrolyte in spite of the presence of Ca^{2+}, the TaF_7^{2-} should be a stronger oxide getter than Ca^{2+}. However, its concentration may be very low (approaching to zero) at the surface during reduction of $TaOF_5^{2-}$.

Since CaO has high energy of formation, Ca^{2+} in the molten salts exhibits strong affinity for oxide ions as clearly demonstrated by Chen *et al.*[23] Furthermore, it has high concentration at the electrode surface. Hence, its constructive role in inhibiting the capturing of O^{2-} by the electro-deposit to form TaO[15] or dissolving the O^{2-} ions away into the bulk electrolyte without allowing them to concentrate at the deposit surface seems highly probable.

4.3 Conproportionation Reaction

Although metallic tantalum is formed by galvanostatic polarization, reverse chronopotentiometry does not show a completely insoluble nature of the product that stays at the electrode to dissolve after current reversal. This is caused by conproportionation reaction.

We have observed two anodic waves (O_3', O_3'') corresponding to a single cathodic wave R_3 (Fig. 7). These results are clearly confirmed by chronopotentiometry. The anodic dissolution exhibits two plateaus corresponding to a single plateau for cathodic deposition from TaF_7^{2-} ions. The product of conproportionation reaction undergoes oxidation and gives rise to an additional anodic plateau. As redox potential for Ta(II)/Ta(V) is much nobler than wave O_3'', the product of conproportionation reaction that oxidizes at wave O_3'' should have lower oxidation state than 2+. Hence, it may be Ta(I). It forms in the vicinity of electrode as a result of reaction between Ta(V) and Ta(0). However, it is unstable in the bulk electrolyte and undergoes disproportionation reaction to form metallic tantalum powder that segregates at the electrolyte surface. In spite of conproportionation reaction, the deposit of metallic tantalum is still present on the electrodes in large quantities as revealed by reverse chronopotentiometry. Nevertheless, this reaction may lead to a significant loss in current efficiency particularly at low deposition rates.

Although disproportionation reaction has been found in electro-deposition of valve metals from molten salts, it has not been reported previously for electro-deposition of tantalum from the fluoride melts (containing LiF, NaF and KF). This suggests a different nature of the melt containing CaF_2. The CaF_2 seems to affect the nature and/or stability/characteristics of fluorotantalate and oxy-fluorotantalate ions in the fluoride melts. Further investigation is necessary to provide a decisive conclusion on this aspect.

4.4 Formation of Intermetallic Compound on Nickel

The deposition of tantalum on nickel follows a slightly different mechanism from tungsten, as shown in Fig. 9. At noble potentials, an intermetallic compound is formed by underpotential deposition of tantalum. After attaining a certain thickness or complete coverage of the surface, the underpotential deposition stops or slows down to extremely low values giving rise to a symmetric peak with very small width in the voltammogram (Fig. 3). Only a single intermetallic compound is found to form by underpotential deposition since no additional peaks are observed that could be associated with the formation of other intermetallic compounds. The potential of its formation is about 0.25 V nobler to that for bulk tantalum. Taxil has reported similar potential for Ni_3Ta.[20]

The intermetallic compound grows significantly during deposition of pure tantalum due to diffusion of tantalum

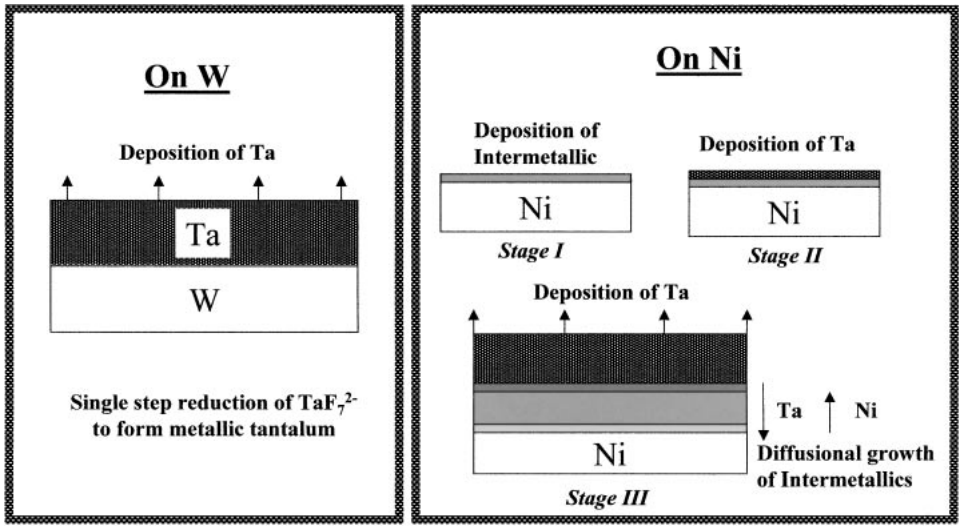

Fig. 9 Mechanism of electro-deposition of tantalum on tungsten and nickel substrates as revealed by electrochemical study.

atoms inward and nickel atoms outward. As a result of growth, other intermetallic compounds are also formed. However, their thickness remains lower than that for the one nucleated by underpotential deposition, as revealed by chronopotentiometry.

Investigations to prepare good coatings on nickel and tungsten substrates in LiF–NaF–CaF_2 on the basis of electrochemical study are underway and will be presented in another paper.[25)]

5. Conclusions

(Electro-deposition on tungsten)

(1) Electro-deposition of tantalum on tungsten has been possible in LiF–NaF–CaF_2 at low current densities, *e.g.*, 2×10^2 A·m^{-2}. A deposit of pure tantalum is formed on tungsten without any entrapped salt. The quality of the interface is not satisfactory, however.

(2) The primary mechanism of electro-reduction of tantalum melt is 5-electron charge transfer from Ta(V) to Ta(0). This happens at a potential of < -0.500 V vs. Ni (quasi-reference electrode) where metallic tantalum is formed from TaF_7^{2-}. A parallel mechanism of electro-reduction of tantalum has also been found to operate with low activity. In this case, the first step is reduction of Ta(V) to Ta(II).

(3) At potentials $< -0.54 \sim -0.55$ V, metallic tantalum is formed from $TaOF_5^{2-}$. The free oxide ions generated by reduction of $TaOF_5^{2-}$ are removed from the surface by a getter, possibly a complex of Ca(II). This characteristic of the melt may facilitate in preparing good coatings with more tolerance against oxide in the melt.

(Electro-deposition on nickel)

(4) Voltametric investigations suggest that an intermetallic compound is formed as a result of underpotential deposition of tantalum and covers the substrate prior to electro-deposition of pure tantalum. This happens at potential ~0.25 V nobler to that for pure tantalum.

(5) The potential shifts to the region of electro-deposition of pure tantalum within a fraction of second at a current density of 2×10^2 A·m^{-2}. Accordingly, the top surface should be covered by pure tantalum in spite of the formation of intermetallic compound. However, the intermetallic compound below pure tantalum continues to grow as a result of diffusion.

(Side Reaction)

(6) The occurrence of conproportionation reaction has also been detected. This takes place in the vicinity of electrode. The corresponding disproportionation reaction occurs in the bulk electrolyte leading to formation of sludge containing powdery tantalum at the salt surface.

Acknowledgements

One of the authors (mm) is grateful to Japan Society of Promotion of Sciences (JSPS) for post-doc fellowship. The authors are thankful to Mr. H. Iijima and Mr. T. Izumi of Showa Cabot Supermetals Co for providing us with Potassium Fluorotantalate powder. The authors are also thankful to Dr. E. G. Polyakov for useful advice.

REFERENCES

1) F. Cardarelli, P. Taxil and A. Savall: Intl. J. Ref. Metals & Hard Materials **14** (1996) 365–381.
2) K. Hashimoto: Mat. Sci. and Eng. **A 198** (1995) 1–10.
3) M. Mehmood, B. P. Zhang, E. Akiyama, H. Habazaki, A. Kawashima, K. Asami and K. Hashimoto: Corros. Sci. **40** (1998) 1–17.
4) M. Mehmood, E. Akiyama, H. Habazaki, A. Kawashima, K. Asami and K. Hashimoto: Corros. Sci. **41** (1999) 1871–1890.
5) M. Mehmood, E. Akiyama, H. Habazaki, A. Kawashima, K. Asami and K. Hashimoto: Corros. Sci. **42** (2000) 361–382.
6) I. Ahmad, T. Spiak and G. E. Janz: J. Appl. Electrochem. **11** (1981) 291–297.
7) S. L. Lee, D. Windover, M. Audio, D. W. Matson and E. D. Mcanahan: Surface and Coating Technology **149** (2002) 62–69.
8) F. Cardarelli, P. Taxil, A. Savall, C. Comninellis, G. Manoli and O. Leclerc: J. Appl. Electrochem. **28** (1998) 245–250.
9) S. Senderoff, G. W. Mellors and W. J. Reinhart: J. Electrochem. Soc. **8** (1965) 266–272.
10) M. Mohamedi, N. Kawaguchi, Y. Sato and T. Yamamura: J. Alloys Compd. **287** (1999) 91–97.
11) Y. Sato, K. Iwabuchi, N. Kawaguchi, H. Zhu, M. Endo, T, Yamamura

and S. Saito: Proc. 10th Intl. Symp. on molten salts **10** (1996) 179–188.
12) D. Inman and S. H. White: J. Appl. Electrochemistry **8** (1978) 375–390.
13) L. P. Polyakova, E. G. Polyakov, A. I. Sorkin and P. T. Stangrit: J. Appl. Electrochem. **22** (1992) 628–637.
14) L. P. Polyakova, E. G. Polyakov, F. Mattiensen, E. Christensen and N. J. Bjerrum: J. Electrochemi. Soc. **141** (1994) 2982–2988.
15) P. Chamelot, P. Palau, L. Massot, A. Savall and P. Taxil: Electrochemica Acta **47** (2002) 3423–3429.
16) N. Kawaguchi: Ph.D. thesis, Tohoku University, 2002.
17) N. Kawaguchi, T. Amano, M. Mehmood, S. Zheng, Y. Sato, T. Yamamura, M. Furusaka and M. Kawai: 2002 Annual Meeting of the Japan Atomic Energy Society, 2002.
18) M. Kawai, K. Kikuchi, H. Kurishita, J. F. Li and M. Furusaka: J. Nucl. Mater. **296** (2001) 312–320.
19) K. Sugimoto: Abstracts of 3rd Workshop on the Materials Technology for Spallation Neutron Source, Mar 14–15, 2002, 6.1 (High Energy Accelerator Research Organization).
20) P. Taxil and J. Mahenc: J. Appl. Electrochem. **17** (1987) 261–269.
21) S. Senderoff, G. W. Mellors and W. J. Reinhart: J. Electrochem. Soc. **112** (1965) 840–845.
22) A. J. Bard and L. P. Faulkner: *Electrochemical Methods (2nd Edition)*, (John Wiley & Sons, Inc., New York, 2001).
23) G. Z. Chen, D. J. Fray and T. W. Farthing: Nature **407** (2000) 361–364.
24) R. A. Bailey, E. N. Balko and A. A. Nobile: J. Inorg. Nucl. Chem. **37** (1975) 971–974.
25) M. Mehmood, N. Kawaguchi, H. Maekawa, Y. Sato, T. Yamamura, M. Kawai and K. Kikuchi: Mater. Trans. **44** (2003) to be submitted.